The International Journal of Robotics Research
30(14) 1775–1788

DOI: 10.1177/0278364911421511
ijr.sagepub.com

On-line frequency adaptation and movement imitation for rhythmic robotic tasks

Tadej Petrič[1], Andrej Gams[1], Auke Jan Ijspeert[2] and Leon Žlajpah[1]

Abstract

In this paper we present a novel method to obtain the basic frequency of an unknown periodic signal with an arbitrary waveform, which can work online with no additional signal processing or logical operations. The method originates from non-linear dynamical systems for frequency extraction, which are based on adaptive frequency oscillators in a feedback loop. In previous work, we had developed a method that could extract separate frequency components by using several adaptive frequency oscillators in a loop, but that method required a logical algorithm to identify the basic frequency. The novel method presented here uses a Fourier series representation in the feedback loop combined with a single oscillator. In this way it can extract the frequency and the phase of an unknown periodic signal in real time and without any additional signal processing or preprocessing. The method determines the Fourier series coefficients and can be used for dynamic Fourier series implementation. The proposed method can be used for the control of rhythmic robotic tasks, where only the extraction of the basic frequency is crucial. For demonstration several highly non-linear and dynamic periodic robotic tasks are shown, including also a task where an electromyography (EMG) signal is used in a feedback loop.

Keywords

Adaptive oscillators, rhythmic movements, adaptive Fourier series

1. Introduction

Performing rhythmic tasks with robots can be accomplished in different ways. Where the interaction between the actuated device and the robot is not crucial, the mechanical properties of the robot can be used to force the behaviour of the actuated device (i.e. the device that the robot is handling) (Sciavicco et al. 2000). For tasks where the dynamic behaviour and response of the actuated device are critical, approaches that adjust the rhythm and behaviour of the robot, in order to achieve synchronization, have to be applied. For example, a feedback loop that locks onto the phase of the incoming signal. Such tasks include swinging of different pendulums (Spong 1995; Furuta 2003), playing with different toys, i.e. the yo-yo (Hashimoto and Noritsugu 1996; Jin and Zacksenhouse 2003; Žlajpah 2006; Jin et al. 2009) or a gyroscopic device called the Powerball (Heyda 2002; Gams et al. 2007; Cafuta and Curk 2008; Petrič et al. 2010), juggling (Schaal and Atkeson 1993; Buehler et al. 1994; Williamson 1999; Ronsse et al. 2007) and locomotion (Ilg et al. 1999; Ijspeert 2008; Morimoto et al. 2008). Rhythmic tasks are also handshaking (Kasuga and Hashimoto 2005; Sato et al. 2007; Jindai and Watanabe 2007) and even handwriting (Hollerbach 1981; Gangadhar et al. 2007). Performing these tasks with robots requires appropriate trajectory generation and foremost precise frequency tuning by determining the basic frequency. We denote the lowest frequency relevant for performing a given task, with the term ‘basic frequency’.

Different approaches have been employed in the past for robotic control of rhythmic tasks. Closed-loop model-based control (An et al. 1988), as a very common control of robotic systems, was applied for juggling (Schaal and Atkeson 1993; Buehler et al. 1994), playing with the yo-yo (Jin and Zackenhouse 2002; Žlajpah 2006) and also for the control of quadruped (Fukuoka et al. 2003) and biped locomotion (Spong and Bullo 2005; Sentis

[1]Department for Automation, Biocybernetics and Robotics, Jožef Stefan Institute, Ljubljana, Slovenia
[2]School of Engineering, Institute of Bioengineering, EPFL – École polytechnique fédérale de Lausanne, Lausanne, Switzerland

Corresponding author:
Tadej Petrič, Department for Automation, Biocybernetics and Robotics, Jožef Stefan Institute, Jamova cesta 39, Ljubljana 1000, Slovenia.
Email: tadej.petric@ijs.si

et al. 2010). Here the basic strategy is to plan a reference trajectory for the robot, which is based on the dynamic behaviour of the actuated device. Standard methods for reference trajectory tracking often assume that a correct and exhaustive dynamic model of the object is available (Jin and Zackenhouse 2002), and their performance may degrade substantially if the accuracy of the model is poor.

An alternative approach to controlling rhythmic tasks is with the use of non-linear oscillators. Oscillators and systems of coupled oscillators are known as powerful modeling tools (Pikovsky et al. 2002) and are widely used in physics and biology to model phenomena as diverse as neuronal signalling, circadian rhythms (Strogatz 1986), inter-limb coordination (Haken et al. 1985), heart beating (Mirollo and Strogatz 1990), etc. Their properties, which include robust limit cycle behaviour, online frequency adaptation (Williamson 1998) and self-sustained limit cycle generation on the absence of cyclic input (Bailey 2004), to name just a few, make them suitable for controlling rhythmic tasks.

Different kinds of oscillators exist and have been used for control of robotic tasks. The van der Pol non-linear oscillator (van der Pol 1934) has successfully been used for skill entrainment on a swinging robot (Veskos and Demiris 2005) or gait generation using coupled oscillator circuits (e.g. Jalics et al. 1997; Tsuda et al. 2007; Liu et al. 2009). Gait generation has also been studied using the Rayleigh oscillator (Filho et al. 2005). Among the extensively used oscillators is also the Matsuoka neural oscillator (Matsuoka 1985), which models two mutually inhibiting neurons. Publications by Williamson (Williamson 1998, 1999) show the use of the Matsuoka oscillator for different rhythmic tasks, such as resonance tuning, crank turning and playing with the slinky toy. Other robotic tasks using the Matsuoka oscillator include control of the giant swing problem (Matsuoka et al. 2005), dish spinning (Matsuoka and Ooshima 2007) and gait generation in combination with central pattern generators (CPGs) and phase-locked loops (Kun and Miller 1996; Kimura et al. 1999; Inoue et al. 2004).

On-line frequency adaptation, as one of the properties of non-linear oscillators (Williamson 1998) is a viable alternative to signal processing methods, such as fast Fourier transform (FFT), for determining the basic frequency of the task. On the other hand, when there is no input into the oscillator, it will oscillate at its own frequency (Bailey 2004). Righetti et al. (2006) have introduced adaptive frequency oscillators, which preserve the learned frequency even if the input signal has been cut. The authors modify non-linear oscillators or pseudo-oscillators with a learning rule, which allows the modified oscillators to learn the frequency of the input signal. The approach works for different oscillators, from a simple phase oscillator (Gams et al. 2009a), the Hopf oscillator, the Fitzhugh–Nagumo oscillator, etc. (Righetti et al. 2006). Combining several adaptive frequency oscillators in a feedback loop allows extraction of several frequency components (Buchli et al. 2008; Gams et al. 2009a). Applications vary from bipedal walking (Righetti and Ijspeert 2006) to frequency tuning of a hopping robot (Buchli et al. 2005). Such feedback structures can be used as a whole imitation system that both extracts the frequency and learns the waveform of the input signal.

Not many approaches exist that combine both frequency extraction and waveform learning in imitation systems (Ijspeert 2008; Gams et al. 2009a). One of them is a two-layered imitation system, which can be used for extracting the frequency of the input signal in the first layer and learning its waveform in the second layer (Gams et al. 2009a). Separate frequency extraction and waveform learning has advantages, since it is possible to independently modulate temporal and spatial features, e.g. phase modulation, amplitude modulation, etc. In addition, a complex waveform can be anchored to the input signal. Compact waveform encoding, such as splines (Thompson and Patel 1987; Miyamoto et al. 1996; Ude et al. 2000), dynamic movement primitives (DMPs) (Schaal et al. 2007), or Gaussian mixture models (GMMs) (Calinon et al. 2007), reduce computational complexity of the process.

Frequency extraction in the first layer in the two-layered system (Gams et al. 2009a) as well as in the one-layered system (Righetti and Ijspeert 2006) is based on adaptive frequency oscillators in a feedback loop. Despite the favorable properties of these systems, there is a considerable drawback in having to determine the basic frequency of the input signal. For complex periodic signals with several frequency components, one has to include a high number of oscillators in the feedback loop and select that with the basic frequency. This is accomplished by a logical algorithm that follows the feedback loop. With a high number of oscillators and when several oscillators tune to the same frequency, it is difficult to select the one with the basic frequency. Since in most practical cases a high number of oscillators is necessary, this problem cannot be avoided.

1.1. Contributions of this paper

The main purpose of this paper is to propose and experimentally evaluate a novel design of the first layer of the two-layered movement imitation system (Gams et al. 2009a), i.e. the movement imitation system based on a pool of frequency oscillators (Righetti and Ijspeert 2006). Using several frequency oscillators in a feedback loop implies having to choose the one with the basic frequency, either by hand or with the use of a logical algorithm. Our novel approach proposed in this paper does not require an additional algorithm to determine the basic frequency of the input signal. We use a single adaptive phase oscillator in a feedback loop, followed by a complete Fourier series approximation, with built-in determination of the coefficients. The combination of an adaptive phase oscillator and the adaptive

Fourier series allows us to extract the basic frequency of the input signal and use it to control rhythmic robotic tasks. With this approach we essentially implement a real-time, on-line and computationally inexpensive adaptive Fourier series analysis.

The usefulness of the proposed system is presented in different rhythmic tasks that require synchronization. These tasks are playing a yo-yo and accelerating a gyroscopic device called the Powerball. These tasks have already been included in several studies (Žlajpah 2006; Gams et al. 2007; Jin et al. 2009; Petric et al. 2009). Most of them rely on complex, specially designed controllers based on the models of the device. The proposed approach simplifies the synchronization between the required motion of the robot and the movement of the device by determining the frequency of the robotic movement from a measurable periodic quantity, which can be the measured torque for the gyroscopic device, or the length of the unwound string for the yo-yo. We show the robustness of the algorithm on a task of synchronizing robotic movement to a measured electromyography (EMG) signal, which usually has a lot of noise. Our approach, which is applicable in prosthetics or for controlling exoskeletons (Ronsse et al. 2010), shows promise for the control of robotic tasks despite the noise and the pseudo-periodic signal produced by an average subject.

This paper is organized as follows. In Section 2 we give a brief description of the original two-layered imitation system with an emphasis on the first layer: the canonical dynamical system (CDS). In Section 3 we describe the novel approach using the Fourier series in the feedback loop. In Section 4 we describe the properties and the possibilities of modulation. We also evaluate the proposed approach in real-world experiments of controlling a yo-yo, accelerating a gyroscopic device, and synchronizing to an EMG signal. The discussion, conclusions and summary are given in Section 5.

2. Two-layered imitation system

The two-layered imitation system was presented in detail by some of us in Gams et al. (2009a). The system can be used for extracting the frequency spectrum of the input signal, learning the waveform of one period, and imitating the desired waveform at an arbitrary frequency. In this section we give a short recap of the system.

The basic system structure is presented in Figure 1. The first layer, i.e. the CDS, is used for frequency extraction. It is based on a set of adaptive frequency oscillators in a feedback loop. The second layer is called the output dynamical system (ODS) and is used for learning and repeating the desired waveform. It is based on DMPs, e.g. Schaal et al. (2007).

The first layer of the system has two major tasks. It has to extract the basic frequency Ω of the input signal and it has

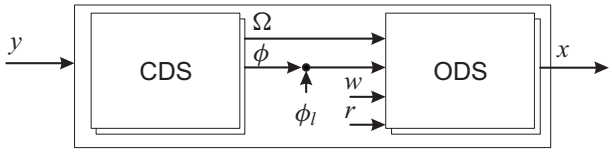

Fig. 1. Two-layered structure of the imitation system. The first layer is the canonical dynamical system (CDS) and the second layer is the output dynamical system (ODS). The input y is a measured quantity and the output is the desired trajectory x of the robot. The input ϕ_l is the additional phase lag and r is the amplitude scaling factor. The system can work in parallel for an arbitrary number of dimensions.

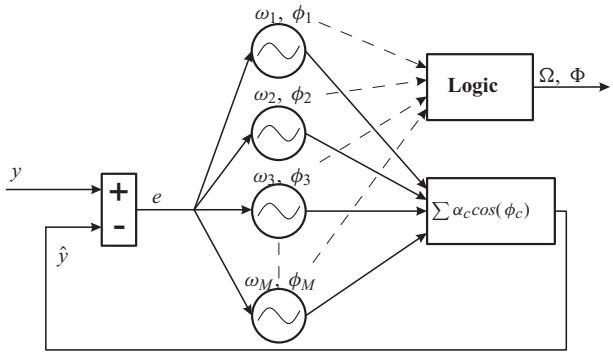

Fig. 2. Feedback structure of M non-linear adaptive frequency oscillators. Note the logical algorithm that follows the feedback loop. A description is given in the text.

to exhibit stable limit cycle behaviour in order to provide the phase signal Φ (Righetti et al. 2006). The basis of the CDS is a set of phase oscillators with an applied learning rule (Buchli and Ijspeert 2004), which makes them adaptive frequency phase oscillators. In order to accurately determine the frequency, the system is combined with a feedback structure as shown in Figure 2. Originally the feedback structure was designed with Hopf oscillators (Buchli et al. 2008). A different oscillator, for example the phase oscillator, can also be modified with the learning rule as described by Righetti et al. (2006).

The feedback structure of M adaptive frequency phase oscillators is governed by the following equations

$$\dot{\phi}_c = \omega_c - K \cdot e \cdot \sin\phi_c, \tag{1}$$

$$\dot{\omega}_c = -K \cdot e \cdot \sin\phi_c, \tag{2}$$

$$e = y - \hat{y}, \tag{3}$$

$$\hat{y} = \sum_{c=1}^{M} \alpha_c \cos\phi_c, \tag{4}$$

$$\dot{\alpha}_c = \eta \cdot e \cdot \cos\phi_c, \tag{5}$$

where K is the coupling strength, ϕ_c, $c = 1, \ldots, M$ are the phases of separate oscillators, y is the input signal, M is the

number of oscillators, α_c is the amplitude associated with the c-th oscillator, and η is the learning constant.

As shown in Figure 2, each of the oscillators in the feedback structure receives the same input signal, i.e. the difference between the input signal and the weighted sum of separate frequency components. Such a feedback structure performs a kind of Fourier analysis. The number of extracted frequencies depends on how many oscillators are used. Because only the basic frequency is of interest, the feedback structure is followed by a logical algorithm, which selects the basic frequency. Determining the correct basic frequency and the phase is crucial, because both form the basis for the ODS and the desired behaviour of the robot/actuated device.

Determining the basic frequency (selecting proper oscillator) from a poll of adaptive frequency oscillators is a challenging task, because there is no straightforward solution. When a large number of oscillators is used, an arbitrary number of them may converge to the same (basic) frequency (see Figure 6 in Section 4.1). If the number is too small, none of them will converge to the basic frequency (see Figure 5 in Section 4.1). To solve these problems, different methods have been proposed. One of them is to choose the oscillator with the highest amplitude (Gams et al. 2009b). Another approach is to choose the first non-zero frequency as it was presented by Gams et al. (2009a). However, such approaches have the drawback that when more than one oscillator converges to (or oscillates around) the same frequency (the amplitudes are in this case similar), the logical algorithm switches between these oscillators. Consequently, the phase will not be smooth, leading to oscillations of the output trajectory. Therefore, we propose a novel method based on a single adaptive frequency oscillator and without a logical algorithm.

3. Canonical dynamical system based on a Fourier series

In this section a novel architecture for the CDS is presented. As the basis of the CDS we use one single adaptive frequency phase oscillator. We combine it with a feed-back structure based on an adaptive Fourier series. The feedback structure is shown in Figure 3.

The feedback structure of an adaptive frequency phase oscillator is governed by

$$\dot{\phi} = \Omega - K \cdot e \cdot \sin\phi, \tag{6}$$

$$\dot{\Omega} = -K \cdot e \cdot \sin\phi, \tag{7}$$

$$e = y - \hat{y}, \tag{8}$$

where K is the coupling strength, ϕ is the phase of the oscillator, e is the input into the oscillator and y is the input signal. If we compare Equations (1), (2) and Equations (6), (7), we can see that the basic frequency Ω and the phase ϕ

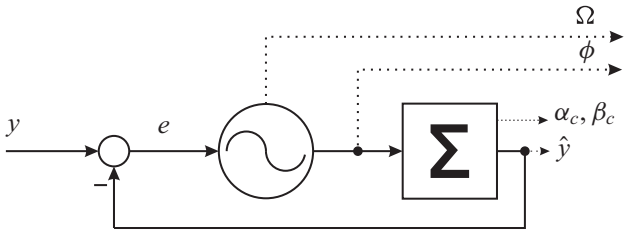

Fig. 3. Feedback structure of an adaptive frequency oscillator combined with dynamic Fourier series. Note that no logical algorithm is needed.

in Equations (6), (7) are clearly defined. The feedback loop signal $\hat{y}$ in (8) is given by the Fourier series

$$\hat{y} = \sum_{c=0}^{M} (\alpha_c \cos(c\phi) + \beta_c \sin(c\phi)), \tag{9}$$

and not by the sum of separate frequency components as in Equation (4). In Equation (9), M is the number of components of the Fourier series and α_c, β_c are the amplitudes associated with the Fourier series governed by

$$\dot{\alpha}_c = \eta \cos(c\phi) \cdot e, \tag{10}$$

$$\dot{\beta}_c = \eta \sin(c\phi) \cdot e, \tag{11}$$

where η is the learning constant and $c = 0, \ldots, M$. As shown in Figure 3, the oscillator input is the difference between the input signal y and the Fourier series $\hat{y}$. Since a negative feedback loop is used, the difference approaches zero when the Fourier series representation $\hat{y}$ approaches the input signal y. Such a feedback structure performs a kind of adaptive Fourier analysis. Formally, it performs only a Fourier series approximation, because input signals may drift in frequency and phase. General convergence remains an open issue. However, we have shown in several numerical and physical examples (Section 4) that our system can converge, i.e. adapt to the basic frequency Ω of the input signal y. The number of harmonic frequency components it can extract depends on how many terms of the Fourier series are used.

As it is able to learn different periodic signals, the new architecture of the CDS can also be used as an imitation system by itself. Once e is stable (zero), the periodic signal stays encoded in the Fourier series, with an accuracy that depends on the number of elements used in Fourier series. The learning process is embedded and is done in real time. There is no need for any external optimization process or other learning algorithm.

It is important to point out that the convergence of the frequency adaptation (i.e. the behaviour of Ω) should not be confused with locking behaviour (Buchli et al. 2008) (i.e. the classic phase locking behaviour, or synchronization, as documented in the literature (Pikovsky et al. 2002)).

The frequency adaptation process is an extension of the common oscillator with a fixed intrinsic frequency. First, the adaptation process changes the intrinsic frequency and not only the resulting frequency. Second, the adaptation has an infinite basin of attraction (Buchli et al. 2008). Third, the frequency stays encoded in the system when the input is removed (e.g. set to zero or $e \approx 0$). In the following numerical experiments the interaction is unidirectional, i.e. the input signal is not affected. In the real-world experiments, the interaction is bidirectional (e.g. behaviour of the yo-yo depends on the behaviour of the robot which again depends on the yo-yo). Our purpose is to show how to apply the approach for control of rhythmic robotic task. For details on analyzing interaction of multiple oscillators, see e.g. Kralemann et al. (2008).

Augmenting the system with an ODS as presented in Gams et al. (2009a) makes it possible to synchronize the movement of the robot to a measurable periodic quantity of the desired task. Namely, the waveform and the frequency of the measured signal are encoded in the Fourier series and the desired robot trajectory is encoded in the ODS. Since the adaptation of the frequency and learning of the desired trajectory can be done simultaneously, all of the system time delays, e.g. delays in communication, sensor measurements delays, etc., are included automatically. Furthermore, when a predefined motion pattern for the trajectory is used, the phase between the input signal and the output signal can be adjusted with a phase lag parameter ϕ_l (see Figure 1). This enables us to either predefine the desired motion or to teach the robot how to perform the desired rhythmic task online.

Even though the CDS by itself can reproduce the demonstration signal, using the ODS allows for easier modulation in both amplitude and frequency, learning of complex patterns without extracting all frequency components and acts as a sort of a filter (Gams et al. 2009a). Moreover, when multiple output signals are needed, only one canonical system can be used with several output systems, which assure that the waveforms of the different degrees of freedom (DOFs) are realized appropriately.

4. System properties

Here we evaluate the proposed CDS based on an adaptive Fourier series. In Section 4.1 the numerical results from the original and the novel architectures are presented. In Section 4.2 real-world experiments on different robots are shown.

4.1. Simulation

In this numerical experiment the proposed architecture for the CDS learns an arbitrary signal. The populating of the frequency spectrum is done without any signal processing or preprocessing, as the whole process of frequency extraction and adaptation of the waveform is completely embedded in the dynamics of the adaptive frequency oscillator combined with the Fourier series. Unless stated otherwise, we use the following parameters in our numerical and real-world experiments: $\eta = 2$, $K = 20$ and $M = 10$.

Frequency adaptation results from the time-varying signals are illustrated in Figure 4. Both approaches are shown: the adaptive Fourier series in a feedback loop and the pool of oscillators in a feedback loop. The top plot shows the signal of the varying frequency, the middle plot shows the frequency adaptation and the bottom plot shows the square error between the target and the extracted frequency ($e_r^2 = (\omega_t - \Omega)^2$ for the proposed system and $e_r^2 = (\omega_t - \omega_c)^2$ for the original system). The signal consists of two parts, a non-stationary signal (a chirp signal) and a stationary signal with two step-changes of the frequency at 30 s and 45 s. We can see that the proposed system is able to adapt to the frequency for both the stationary and the changing target frequency. Compared with the system with a pool of oscillators proposed in Gams et al. (2009a), we can see that both systems behave similarly. However, in this particular case, a single adaptive oscillator in a feedback loop is enough, because the input signal is purely sinusoidal and has only one frequency component.

Figure 5 shows the frequency adaptation results for time- and shape-varying signals, which have several frequency components. The input signal consists of three parts: a periodic pulse signal, a sinusoidal signal, and a sawtooth wave signal. The transition between the signal parts is instantaneous for both frequency and waveform, which is easily achieved in simulation, but also happens in real-word scenarios, e.g. when switching between different sensor systems. Nevertheless, we can see that after the change of the input signal, the output frequency stabilizes at the target frequency.

The approximation of the input signal ($\hat{y}_o$), using the original approach, is marked with a dotted line. We can see that a single adaptive frequency oscillator in a feedback loop is not enough when the original approach (Gams et al. 2009a) is used. However, when the novel approach is used, only one adaptive frequency oscillator is enough. As can be seen from the bottom plots in Figure 5, the input signal y and the feedback signal of our proposed approach $\hat{y}$ are very well matched. The approximation error depends only on the size of the Fourier series M.

In addition to the use for non-stationary signals, e.g. chirp signals, coping with the change in frequency of the input signal proves to be useful when adapting to the frequency of a measured periodic signal, e.g. the force feedback when playing the Powerball (see Figure 15).

Another comparison with the original approach as proposed in Buchli et al. (2008) is given in Figure 6. In the original approach, if there are not enough oscillators to encode the input signal, the system will learn only the strongest frequency components. Thus, the output signal will only be

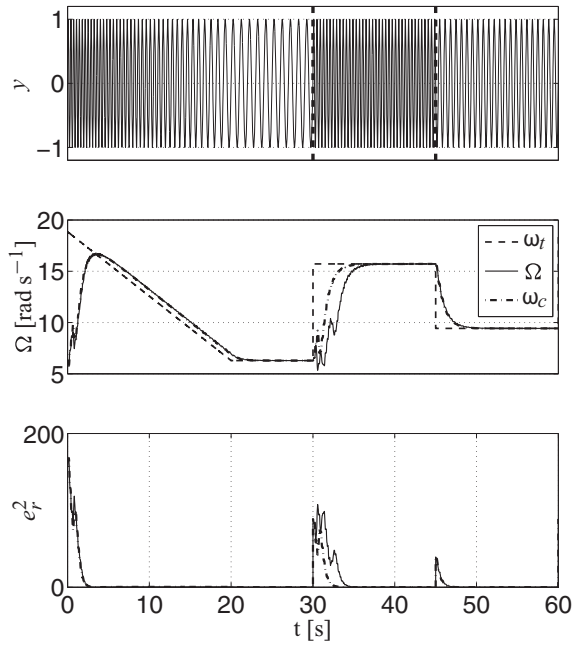

Fig. 4. Typical convergence of an adaptive frequency oscillator combined with an adaptive Fourier series (—) compared with the previous system of a poll of c oscillators (-.-). In this case $c = 1$. The input is a periodic signal ($y = \sin(\omega_t t)$, with $\omega_t = (6\pi - \pi/5t)$ rad s^{-1} for $t < 20$ s, followed by $\omega_t = 2\pi$ rad s^{-1} for $t < 30$ s, followed again by $\omega_t = 5\pi$ rad s^{-1} for $t < 45$ s and finally $\omega_t = 3\pi$ rad s^{-1}). Frequency adaptation is presented in the middle plot, starting at $\Omega_0 = \pi$ rad s^{-1}, where ω_t is given by the dashed line and Ω by the solid line. The square error between the target and the extracted frequency is shown in the bottom plot. We can see that the adaptation is successful for non-stationary signals, step changes and stationary signals.

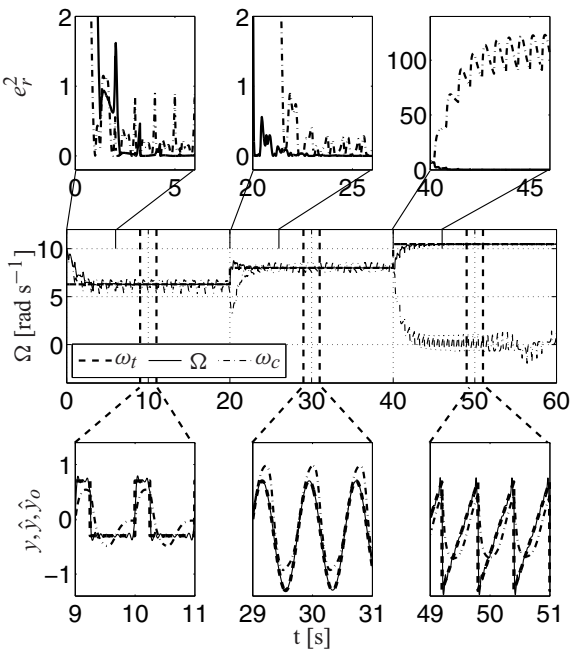

Fig. 5. Typical convergence of an adaptive frequency oscillator combined with an adaptive Fourier series. The input is a periodic signal with different waveforms and frequencies. Frequency adaptation is presented in the middle plot. The bottom plots show close-ups. The input signal y is dashed, the adaptive Fourier series approximation $\hat{y}$ is solid, and the pool of oscillators (one oscillator) approximation $\hat{y}_o$ is dotted. The square error between the target and the extracted frequency is shown in the top plots.

a rough approximation. However, if there are more oscillators than the frequency components to learn, either some of them will not converge to any frequency component, or the same frequency components will be coded by several oscillators, as shown in the top plot in Figure 6, where a pool of 10 oscillators was used ($c = 10$). In this particular example, five of the oscillators converge to the basic frequency of the signal. Selecting the proper oscillator from the pool is a difficult task and requires a complex logical algorithm.

On the other hand, using our new approach, where the feedback is encoded with a Fourier series, the oscillator converges to the basic frequency of the input signal. Therefore, the basic frequency and the phase are clearly defined. Furthermore, the approximation and the convergence of the feedback signal is quicker in this example (solid line), as shown in the two bottom rows of plots in Figure 6. The bottom row shows the errors of both approximations. The errors are only similar after more than 350 s.

Figure 7 shows the convergence of coefficients. For clarity, in this particular example, the size of the Fourier series was three ($M = 3$). The input signal itself is of three parts, a periodic pulse signal, a sinusoidal signal and a sawtooth wave signal, all with the same constant frequency ($\Omega = 8$ rad s^{-1}). The transition between the signal parts is instantaneous.

After the instantaneous change of the input signal, the Fourier series coefficients converge to constant values. We can see in the top plot that the α_0 coefficient converges to the exact value of the input signal offset, e.g. 1 in the case of the periodic pulse signal, 0.5 in the case of the sinusoidal signal, and -0.5 in the case of the sawtooth signal.

The speed of convergence in general depends on the coupling strength K (see Equation (6) and (7)) and the initial condition of the adaptive frequency oscillator (Righetti and Ijspeert 2006; Gams et al. 2009a). In general, the proposed system usually converges to the frequency component of the input signal with the highest amplitude in the power spectrum, which is in practice usually also the basic frequency. Figure 8 shows the result of frequency adaptation to signals with several frequency components with different amplitudes. In this particular example we can see that the system always converged to the first frequency component, even if the harmonics of the basic frequency have higher amplitudes.

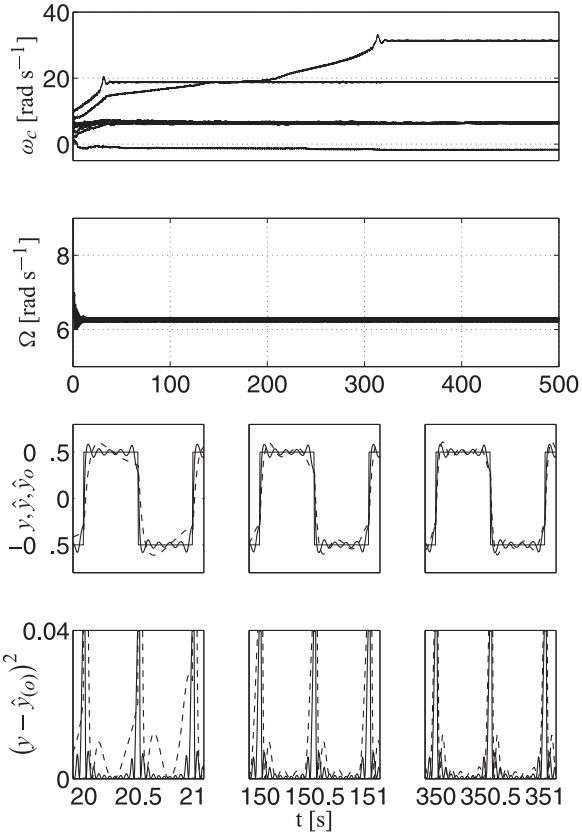

Fig. 6. Comparison between using a pool of adaptive oscillators and our proposed approach. The first plot shows the evolution of frequency distribution using a pool of 10 oscillators. The second plot shows the extracted frequency using our proposed approach. The comparison of the target and the approximated signals is presented in the third plot. The thin solid line presents the input signal y, the thick solid line presents our new proposed approach $\hat{y}$ and the dotted line presents the original approach with a pool of adaptive oscillators $\hat{y}_o$. The square difference between the input and the approximated signals is presented in the bottom plot.

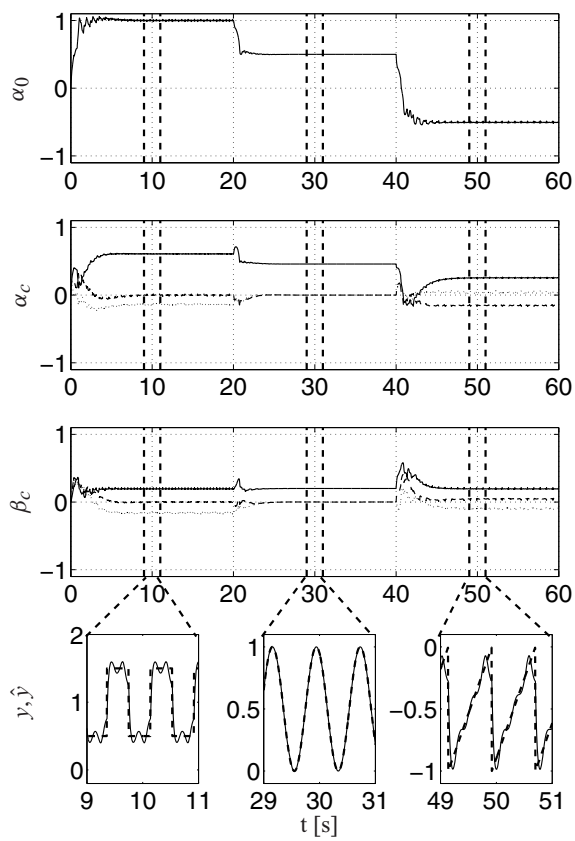

Fig. 7. Typical coefficient convergence of an adaptive frequency oscillator combined with an adaptive Fourier series, driven by a periodic signal with different waveforms and a constant frequency ($\Omega = 8$ rad s^{-1}). The α_0 adaptation is presented in the top plot, α_c is presented in second plot and β_c is presented in third plot, where $c = 1, 2, 3$. The comparison between the input signal y and the approximation $\hat{y}$ is shown in the bottom plot.

An interesting aspect of our system is also the ability to deal with non-stationary input signals and to adapt to changes of the input signal in both frequency and waveform. Figure 9 shows the results of adapting to the signal where the waveform of the input signal introduces a frequency halving. We can see that when the oscillations of the lowest frequency component increase (top plot), the oscillator adapts to a new basic frequency (2π). When learning the frequency of multi-frequency input signals, one should expect convergence to any frequency component of the input signal, depending on the initial conditions and the amplitude of the frequency component. This means that a system in general can have more than one attractor, each with its own basin of attraction (Pikovsky et al. 2002). In Righetti et al. (2006) the authors showed how to analytically predict different basins of attraction for similar system.

Our system can also cope with pseudo-periodic signals. A strange attractor of the Lorenz system is defined by

$$\dot{a} = -\sigma a + \sigma b, \tag{12}$$

$$\dot{b} = -ac + ra - b, \tag{13}$$

$$\dot{c} = ab - \beta c, \tag{14}$$

where $\sigma = 10$, $r = 28$ and $\beta = \frac{8}{3}$ (parameters from which the system produces a strange attractor) (Strogatz 1994). The Fourier spectrum of the c variable indicates two major frequency components (Righetti et al. 2006). The first at frequency zero, since the average of c, $\bar{c} \neq 0$ and the second at ~ 1.3 Hz. Here the c variable is used as the input signal into our system.

Figure 10 shows the result of frequency adaptation to the pseudo-periodic input signal. Even though the input signal (see the top plot in Figure 10) has a strong zero-frequency

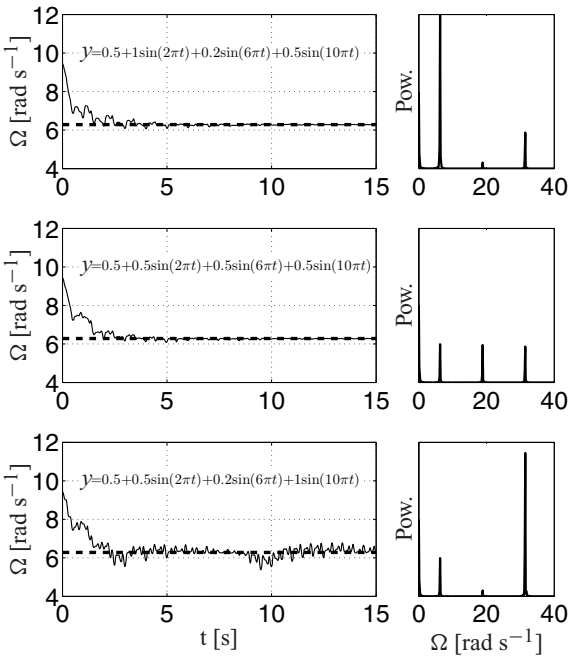

Fig. 8. Frequency adaptations of the proposed canonical dynamical system to the input signal $y(t) = a_0 + a_1 \sin(2\pi t) + a_2 \sin(6\pi t) + a_3 \sin(10\pi t)$, with the initial condition of the adaptive frequency oscillator at $\Omega_0 = 3\pi$ are presented in the left-hand plots. Frequency spectrums are shown in the right-hand plots. We can see that the system successfully adapts to the basic frequency. The oscillator parameters are $\eta = 2$ and $K = 10$.

component, the system is able to extract the frequency, i.e. $\Omega \simeq 8.27$ rad s^{-1}, which corresponds to the intrinsic frequency of the oscillator of $\sim$ 1.3 Hz. Thus, our system has learned the pseudo-frequency of the Lorenz attractor. As this is not a strictly periodic signal, Ω oscillates, following the constant changing pseudo-frequency of the attractor.

4.2. Experimental evaluation

To further illustrate the properties of the proposed approach we implemented it on different robot systems performing different tasks. These tasks are playing with a yo-yo and playing with the Powerball. In the end we also show the results of on-line frequency adaptation to an EMG signal measured on a human muscle. In the cases of the Powerball and yo-yo a Mitsubishi PA-10 robot was used, and for the adaptation to an EMG signal a Fujitsu HOAP-3 robot was used. With the real experiments we showed that the proposed system can be applied to a mechanical system, which is usually subject to a variety of disturbances, i.e. noise and delays.

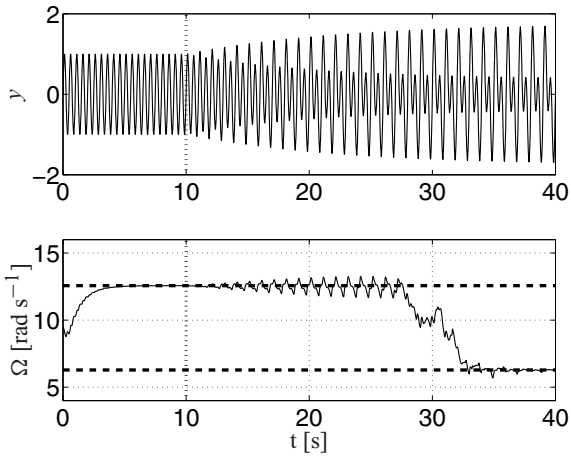

Fig. 9. Frequency adaptation results of the proposed canonical dynamical system to the changes of input signal from $y(t) = \sin(4\pi t)$ to $y(t) = \sin(4\pi t) + (1 - e^{-0.035t}) \sin(2\pi t)$ starting at 10 s (top plot), with the initial condition of the adaptive frequency oscillator at $\Omega_0 = 3\pi$ are presented in the bottom plot. We can see that when the oscillations of the frequency are large enough, the extracted frequency adapts to the new frequency (2π). The parameters are $\eta = 1$ and $K = 10$.

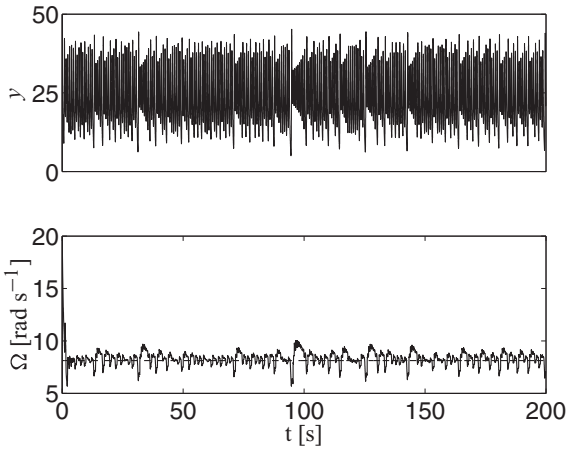

Fig. 10. Frequency adaptations results (bottom plot) of the proposed canonical dynamical system to the pseudo-periodic input signal (top plot), with the initial condition of the adaptive frequency oscillator at $\Omega_0 = 20$ rad s^{-1}. We can see that the system can correctly learn the pseudo-frequency of the Lorenz system. The parameters are $\eta = 2$ and $K = 3$.

4.2.1. Application to a robotic yo-yo The task of playing with a yo-yo requires synchronized movement of the robot and the device. With this experiment we show the ability of the system to work in a bidirectional interaction setting, adaptive properties and robustness of the proposed control strategy.

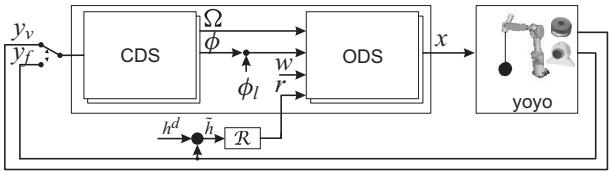

Fig. 11. Proposed two-layered structure of the control system for controlling the peak height of the yo-yo. The input is either the force y_f or the visual feedback y_v.

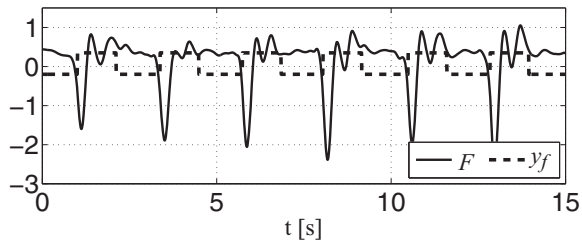

Fig. 12. Modifying the measured force spike F into a short pulse y_f.

Using a robot to play with a yo-yo can be achieved in different ways, depending on what one can measure (Žlajpah 2006; Gams et al. 2009b; Jin et al. 2009). It can be the length of the unwound string, which can be effectively measured using a vision system, or the force in the string, which can be measured by a force sensor. As described in Žlajpah (2006), using the vision is also the usual way humans play with a yo-yo, even though approaches using only the measured force were described (e.g. Jin et al. 2009). With the proposed strategy playing the yo-yo can be accomplished with either the force feedback or the visual feedback. Furthermore, the proposed system is able to synchronize the movement of the robot and the yo-yo even if the input signal is changed during the experiment from one measured quantity to another, i.e. from force to vision feedback or vice versa.

We performed the experiment on a Mitsubishi PA-10 robot. A JR-3 force/torque sensor was attached to the top of the robot to measure the impact force of the yo-yo. A 60 Hz USB camera was used to measure the length of the unwound string by measuring the distance between the yo-yo and the gripper. The two-layered imitation system with the proposed CDS was implemented in Matlab/Simulik. The control scheme is presented in Figure 11. The imitation system, which is based on an adaptive frequency oscillator combined with a dynamic Fourier series in the first layer, and a DMP in the second layer provides the desired trajectory for the robot. The motion of the robot is constrained to up–down motion using inverse kinematics. Either the length of the string or the string force can be used as the input. Since a measurable force difference appears only as a spike when the bottom impact of the yo-yo occurs, we modify the force signal by using the measured spike to create a short pulse as shown in Figure 12. Even though we pre-process the waveform of the signal, no pre-processing in the sense of determining the frequency or the width of the processing window is done.

To perform the task, we first determined the waveform of the required motion pattern. We chose the motion pattern described in Žlajpah (2006). As described in Žlajpah (2006), such a motion pattern satisfies the required velocity and acceleration criteria for playing the yo-yo (upper jerk before the yo-yo hits the bottom). The hand motion pattern was encoded into the output dynamic system.

The frequency of the task depends on the parameters of the yo-yo, and on how high the yo-yo rolls up along the string. The height can be influenced by the amplitude of the hand motion, which can be easily modified using the amplitude parameter r of the motion, see Figure 11. A PI controller was used to control the peak height of the yo-yo. The controller is given by

$$u(t) = k_p \tilde{h}(t) + k_i \int \tilde{h}(t)\, dt, \tag{15}$$

where $k_p = 2$, and $k_i = 0.4$ were determined empirically and $\tilde{h}(t)$ is given by the difference between the desired maximum height h_d and the current maximum height h of the yo-yo.

Figure 13 shows the results of frequency adaptation and the yo-yo height during the experiment. As we can see the frequency of the imitated motion quickly adapted to the motion of the yo-yo and stable motion was achieved. At approximately 32 s the input into the imitation system was switched from visual feedback to force feedback, and vice versa at 63 s. Some oscillations in the frequency can be observed at that point, because the system has to adapt to the new waveform of the input signal. Despite the changes in the input signal, the imitation system still manages to extract the correct frequency and the robot motion returns to steady-state oscillations. For a video of the robotic yo-yo, see Extension 1.

As far as we know, this is the first system which has the capability of playing the yo-yo by force feedback or by vision feedback without changing the system parameters. Furthermore, switching from one to the other measured quantity can even be done during the experiment. This shows that the proposed system is, based on the experiments conducted, robust to some changes in the input signal shape.

4.2.2. Application to robotic Powerball The Powerball is the commercial name for a gyroscopic device that exhibits rotor spin-up when operated appropriately. The device has a rotor with two underactuated DOFs, which can be actuated by the appropriate motion of human or robot wrist axes (see Petrič et al. 2010, for details). After the initial spin, applying appropriate motion and torques to the housing leads to

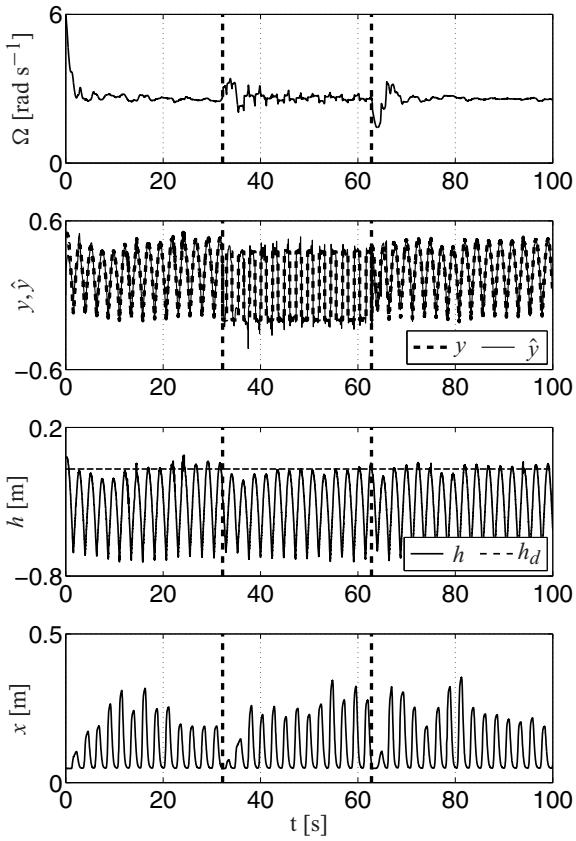

Fig. 13. Extracted frequency Ω in the top plot, signal adaptation $\hat{y}$ in the second plot, height h of the yo-yo in the third plot and robot trajectory x in the bottom plot. At 32 s the input signal is switched from visual feedback to force feedback and at 63 s the situation is reversed. Yo-yo parameters in this case are axle radius $r_a = 0.01$ m and mass $m = 0.26$ kg.

a spin-up of the rotor. Finding these torques intuitively is an easy task for human operators, but a complex task for a technical consideration, for example, in robotics.

The task of accelerating the Powerball with a robot includes some major challenges. First the robot and the device have to be synchronized. Next the achieved rotor speeds should be comparable to an average human operator. With our proposed system, playing with the Powerball can be accomplished by using a torque feedback loop. The experiment was performed on a Mitsubishi PA-10 robot with a mounted force/torque sensor. A gripper with the Powerball was attached to the JR3 sensor and a reed relay was installed into the gripper to measure the rotational speed of the rotor.

To accelerate the device we implemented the two-layered imitation system with the proposed CDS in Matlab/Simulink as presented in Figure 14. In this particular experiment only the two robot's wrist DOFs were used to resemble human motion as explained in Gams et al. (2007).

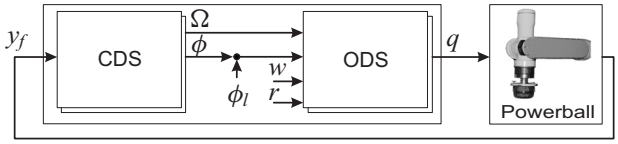

Fig. 14. Proposed two-layered structure of the control system for accelerating gyroscopic device. The input is the measured torque y_f.

Both joints have the same motion pattern (sinusoidal) with a phase difference between them at $\phi_l = \pi/2$. Therefore, the device was travelling in a circle, which satisfies the required kinematic criteria for accelerating the gyroscopic device (Petrič et al. 2010).

The results of accelerating the device are presented in Figure 15, where both the simulation and the real-world experiments are compared. The top plot shows the achieved rotor velocity where the initial spin velocity was set to 500 rad s^{-1}. We can see that in the beginning the rotor is decelerating until the control system adapts to the rotor precession frequency. As soon as it adapts, the rotor starts to accelerate until it reaches the physical limitations of the system. The limitations in the simulation were set to resemble experiments on a Mitsubishi PA-10 robot. The phase angle ϕ between the robot motion and the device is almost constant during the acceleration (see the bottom plot in Figure 15). For a video of the robotic Powerball, see Extension 2.

In the middle plot the adaptation of the frequency Ω is shown. It also represents the precession speed of the gyroscopic device, when the rotor is rolling without sliding. In this case the precession speed Ω is proportional to the spin speed ω. According to Petrič et al. (2010) the ratio between these speeds is 32.

The bottom diagram shows the phase angle ϕ, which defines the relationship between the motion of the robot and the motion of the device. It is important that the phase angle ϕ is close to zero, because the least amount of energy dissipates at $\phi = 0$ and the acceleration is highest (Petrič et al. 2010).

The experiment showed that the implemented control worked well in the simulation and in the experiment. The best result achieved was 1,367 rad s^{-1} (13,054 rpm) before reaching the physical limitation of our robot, i.e. the measured force at the top of the robot exceeds 125 N, while the Mitsubishi PA-10 allows payload up to 100 N. The results demonstrate the ability of our control strategy to adapt the behaviour of a robot to a changing input frequency.

4.2.3. Application of EMG signals for controlling periodic motion In this section we show the results of synchronizing robot movement to an EMG signal measured from the human biceps muscle (see Figure 16). The purpose

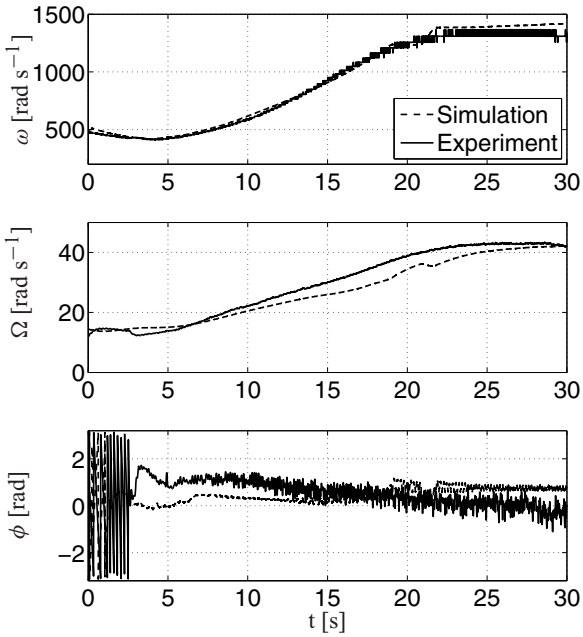

Fig. 15. Rotor velocity ω during acceleration in the top plot, extracted frequency Ω in the middle plot and phase angle ϕ between the motion of the device and the motion of the robot in the bottom plot.

of this experiment is to show frequency extraction from a signal with a low signal-to-noise ratio. This type of application can be used for control of periodic movements of limb prosthesis (Castellini and van der Smagt 2009) or exoskeletons.

In our experimental setup we attached an array of three electrodes (Motion Control Inc.) over the biceps muscle of a subject and asked the subject to flex his arm when he hears a beep. The frequency of beeping was 1 Hz from the start of the experiment, then changed to 0.5 Hz after 30 s, and then back to 1 Hz after an additional 30 s. Figure 17 shows the results of frequency extraction (third plot) from the envelope (second plot) of the measured EMG signal (top plot). The bottom plots show the power spectrums of the input signal from 0 s to 30 s, from 30 s to 60 s and from 60 s to 90 s, respectively. The power spectrums were determined off-line. For a video of the application of EMG signals for controlling periodic motion, see Extension 3.

Figure 18 show the comparison between the envelope of the measured and rectified EMG signal (y) and the generated movement signal (x). As we can see, the proposed system matches the desired movement of the robot with the measured movement.

5. Conclusions

We have presented a new architecture for the CDS which is a part of a two-layered imitation system, but can be used as an imitation system by itself as shown in Section 4.1. The dynamical system, which is used to extract the frequency of the input signal, is composed of an adaptive frequency oscillator combined with a dynamic Fourier series. We have shown that our system extracts the phase and associated frequency and Fourier coefficients which closely reproduce signals form several numerical and physical systems. We expect that our results would generalize, and that our system would be able to extract the frequency, the phase and the Fourier series coefficients of an unknown periodic signal. The process runs in real time without any additional pre-processing of the input signal in the sense of extracting the frequency, such as FFT, sliding windows, etc. Integrating this system into the imitation system based on DMPs enables a simple and computationally inexpensive control of rhythmic tasks with at least one measurable periodic quantity. In comparison with the original canonical system (Righetti and Ijspeert 2006; Gams et al. 2009a) our novel system allows easier extraction of the basic frequency of the input signal in the sense of frequency extraction. In comparison with movement execution approaches with other nonlinear oscillators, such as the van der Pol oscillator (Veskos and Demiris 2005) or the Matsuoka oscillator (Williamson 1998), the greatest advantage of our system is that it learns the frequency of the input signal and maintains it even if the input signal has been cut.

We also presented the use of the imitation system to perform different rhythmic tasks that require synchronization with the controlled device. We have shown that the proposed system can, under certain initial conditions, achieve synchronized movement of the robot and the device. General stability of the control system remains an open issue. On the other hand, Righetti et al. (2006) have shown how to analytically predict the convergence and the output of a pool of oscillators, which are the basic for our frequency extraction, based on the initial conditions.

For playing the yo-yo, we have shown that the information on how high the yo-yo rolls up along the string, or the force feedback are enough to achieve stable performance. Furthermore, we also showed that the system has the capability of changing the measured quantity in a single experiment without losing the synchronization between the robot and the yo-yo. This surpasses the results of previous experiments (Jin and Zacksenhouse 2003; Žlajpah 2006; Jin et al. 2009) in repeatability and ability of switching from one measurable quantity to another in a single experiment, which shows greater robustness of the described approach. This experiment also demonstrates the ability of the system to work in bidirectional interaction settings. For playing the Powerball we have shown that the system is able to adapt and to maintain synchronization when the input frequency is changing. This allow us to achieve very fast acceleration without any introduced knowledge on maintaining the phase as in Gams et al. (2007), and high rotor speeds of the

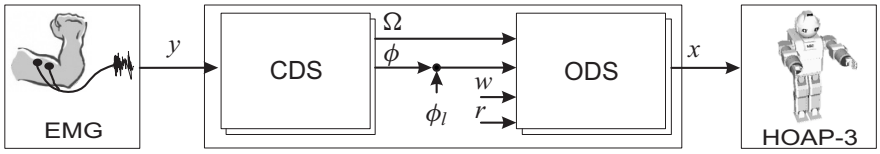

Fig. 16. Proposed two-layered structure of the control system for synchronizing the robotic motion to the EMG signal.

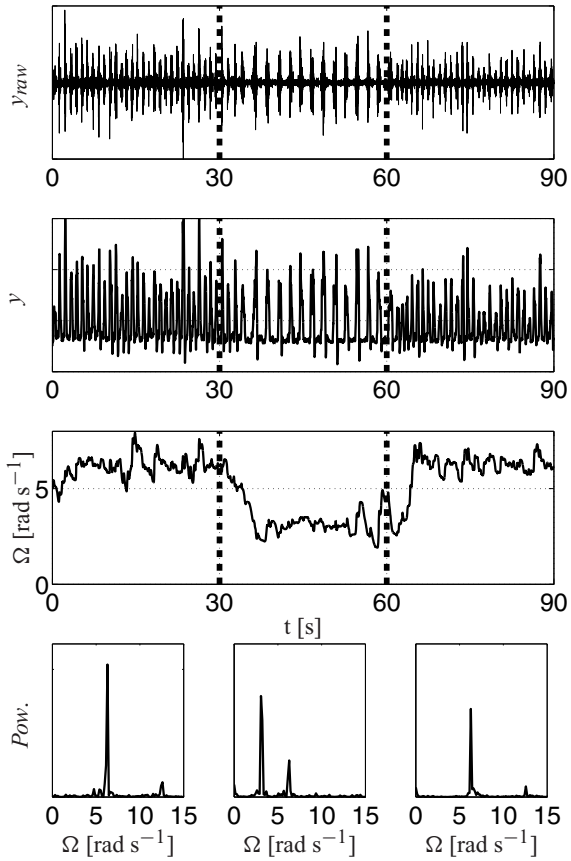

Fig. 17. Raw EMG signal in the top plot and envelope of the EMG signal, which is the input into the proposed system, in the second plot. The third plot shows the extracted frequency Ω. The bottom plots show the power spectrum of the signal at different times (determined off-line).

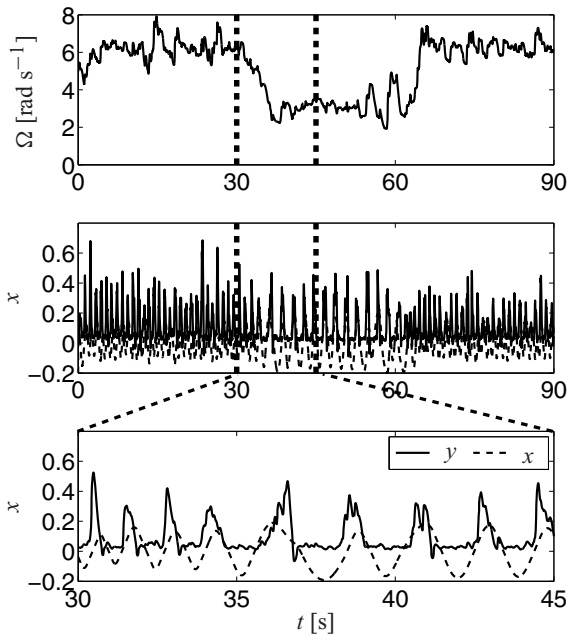

Fig. 18. Extracted frequency in the top plot. Comparison between the envelope of the rectified EMG signal (y), which is used as the input into the frequency-extraction system, and the generated output trajectory for the robot arm (x) is shown in the middle and bottom plots.

Powerball. We have also shown that the system can easily be applied to different robots. Finally, we have shown the applicability of the system to extract the frequency of human movement using EMG. Such strategy has the potential to be applied in controlling prosthetic limbs and exoskeletons (Castellini and van der Smagt 2009; Ronsse et al. 2010).

We believe that our proposed method is suitable to include more complex control. For example, it could be easily integrated into a more general controller for humanoid robots, exoskeleton suits or prosthetic limbs. Future work will include integration of more complex sensory feedback. We will also study how to integrate the proposed system with more advanced force/torque control techniques to control the compliance, stability and posture of a humanoid robot.

Funding

This research received no specific grant from any funding agency in the public, commercial, or not-for-profit sectors.

References

An C, Atkeson C and Hollerbach J (1988) *Model-based Control of A Robot Manipulator*. Cambridge, MA: The MIT Press.

Bailey A (2004) *Biomimetic Control with a Feedback Coupled Nonlinear Oscillator: Insect Experiments, Design Tools, and Hexapedal Robot Adaptation Results*. PhD Thesis, Stanford University.

Buchli J and Ijspeert A (2004) A simple, adaptive locomotion toy-system. In Schaal S, Ijspeert A, Billard A, Vijayakumar S, Hallam J and Meyer J (eds), *From Animals to Animats 8. Proceedings of the Eighth International Conference on the Simulation of Adaptive Behavior (SAB'04)*. Cambridge, MA: The MIT Press, pp. 153–162.

Buchli J, Righetti L and Ijspeert AJ (2005) A dynamical systems approach to learning: A frequency-adaptive hopper robot. In Capcarrere MS, Freitas AA, Bentley PJ, Johnson CG and Timmis J (eds), *Advances in Artificial Life* (*Lecture Notes in Computer Science*, Vol. 3630). Berlin: Springer, pp. 210–220.

Buchli J, Righetti L and Ijspeert AJ (2008) Frequency analysis with coupled nonlinear oscillators. *Physica D: Nonlinear Phenomena* 237: 1705–1718.

Buehler M, Koditschek D and Kindlmann P (1994) Planning and control of robotic juggling and catching tasks. *The International Journal of Robotics Research* 13: 101–118. http://ijr.sagepub.com/content/13/2/101.abstract.

Cafuta P and Curk B (2008) Control of nonholonomic robotic load. In *10th IEEE International Workshop on Advanced Motion Control, 2008. AMC '08*, pp. 631–636.

Calinon S, Guenter F and Billard A (2007) On learning, representing, and generalizing a task in a humanoid robot. *IEEE Transactions on Systems, Man, and Cybernetics, Part B: Cybernetics* 37: 286–298.

Castellini C and van der Smagt P (2009). Surface EMG in advanced hand prosthetics. *Biological Cybernetics* 100: 35–47.

Filho ACdP, Dutra MS and Raptopoulos LSC (2005) Modeling of a bipedal robot using mutually coupled rayleigh oscillators. *Biological Cybernetics* 92: 1–7. DOI: 10.1007/s00422-004-0531-1.

Fukuoka Y, Kimura H and Cohen AH (2003) Adaptive dynamic walking of a quadruped robot on irregular terrain based on biological concepts. *The International Journal of Robotics Research* 22: 187–202. http://ijr.sagepub.com/content/22/3-4/187.abstract.

Furuta K (2003) Control of pendulum: from super mechano-system to human adaptive mechatronics. In *Proceedings 42nd IEEE Conference on Decision and Control, 2003*, Vol. 2, pp. 1498–1507.

Gams A, Ijspeert AJ, Schaal S and Lenarcic J (2009a) On-line learning and modulation of periodic movements with nonlinear dynamical systems. *Autonomous Robots* 27: 3–23.

Gams A, Petrič T and Žlajpah L (2009b) Controlling yo-yo and gyroscopic device with nonlinear dynamic systems. In *18th International Workshop on Robotics*, Alpe-Adria-Danube Region, Brasov, Romania, 25–27 May 2009.

Gams A, Žlajpah L and Lenarčič J (2007) Imitating human acceleration of a gyroscopic device. *Robotica* 25: 501–509.

Gangadhar G, Joseph D and Chakravarthy V (2007) An oscillatory neuromotor model of handwriting generation. *International Journal on Document Analysis and Recognition* 10: 69–84. DOI: 10.1007/s10032-007-0046-0.

Haken H, Kelso JAS and Bunz H (1985) A theoretical model of phase transitions in human hand movements. *Biological Cybernetics* 51: 347–356. DOI: 10.1007/BF00336922.

Hashimoto, K. and Noritsugu, T. (1996). Modeling and control of robotic yo-yo with visual feedback. In *Proceedings 1996 IEEE International Conference on Robotics and Automation*, Vol. 3, pp. 2650–2655.

Heyda PG (2002) Roller ball dynamics revisited. *American Journal of Physics* 70: 1049–1051. http://link.aip.org/link/?AJP/70/1049/1.

Hollerbach JM (1981) An oscillation theory of handwriting. *Biological Cybernetics* 39: 139–156. DOI: 10.1007/BF00336740.

Ijspeert AJ (2008) Central pattern generators for locomotion control in animals and robots: A review. *Neural Networks* 21: 642–653. http://www.sciencedirect.com/science/article/B6T08-4SH6B9F-2/2/2e0a2fdad02d315becc218a6602f054d.

Ilg W, Albiez J, Jedele H, Berns K and Dillmann R (1999) Adaptive periodic movement control for the four legged walking machine BISAM. In *Proceedings 1999 IEEE International Conference on Robotics and Automation*, Vol. 3, pp. 2354–2359.

Inoue K, Ma S and Jin C (2004) Neural oscillator network-based controller for meandering locomotion of snake-like robots. In *Proceedings 2004 IEEE International Conference on Robotics and Automation. ICRA '04*, Vol. 5, pp. 5064–5069.

Jalics L, Hemami H and Zheng Y (1997) Pattern generation using coupled oscillators for robotic and biorobotic adaptive periodic movement. In *Proceedings 1997 IEEE International Conference on Robotics and Automation*, Vol. 1, pp. 179–184.

Jin H-L, Ye Q and Zacksenhouse M (2009) Return maps, parameterization, and cycle-wise planning of yo-yo playing. *Transactions on Robotics* 25: 438–445.

Jin H-L and Zackenhouse M (2002) Yoyo dynamics: Sequence of collisions captured by a restitution effect. *Journal of Dynamic Systems, Measurement, and Control* 124: 390–397. http://link.aip.org/link/?JDS/124/390/1.

Jin H-L and Zacksenhouse M (2003) Oscillatory neural networks for robotic yo-yo control. *IEEE Transactions on Neural Networks* 14: 317–325.

Jindai M and Watanabe T (2007) Development of a handshake robot system based on a handshake approaching motion model. In *2007 IEEE/ASME International Conference on Advanced Intelligent Mechatronics*, pp. 1–6.

Kasuga T and Hashimoto M (2005) Human–robot handshaking using neural oscillators. In *Proceedings of the 2005 IEEE International Conference on Robotics and Automation. ICRA 2005*, pp. 3802–3807.

Kimura H, Akiyama S and Sakurama K (1999) Realization of dynamic walking and running of the quadruped using neural oscillator. *Autonomous Robots* 7: 247–258. DOI: 10.1023/A:1008924521542.

Kralemann B, Cimponeriu L, Rosenblum M, Pikovsky A and Mrowka R (2008) Phase dynamics of coupled oscillators reconstructed from data. *Physical Review E* 77: 066205.

Kun A and Miller IWT (1996) Adaptive dynamic balance of a biped robot using neural networks. In *Proceedings 1996 IEEE International Conference on Robotics and Automation*, Vol. 1, pp. 240–245.

Liu C, Chen Q and Zhang J (2009) Coupled van der Pol oscillators utilised as central pattern generators for quadruped locomotion. In *Proceedings of the Chinese Control and Decision Conference, 2009. CCDC '09*, pp. 3677–3682.

Matsuoka K (1985) Sustained oscillations generated by mutually inhibiting neurons with adaptation. *Biological Cybernetics* 52: 367–376. DOI: 10.1007/BF00449593.

Matsuoka K, Ohyama N, Watanabe A and Ooshima M (2005) Control of a giant swing robot using a neural oscillator. In *Proceedings of ICNC*, Vol. 2, pp. 274–282.

Matsuoka K and Ooshima M (2007) A dish-spinning robot using a neural oscillator. *International Congress Series* 1301: 218–221. http://www.sciencedirect.com/science/article/B7581-4NYJD61-1W/2/4f97ffac6fcbc64aadcfcb70fc6ed5fc.

Mirollo RE and Strogatz SH (1990) Synchronization of pulse-coupled biological oscillators. *SIAM Journal of Applied Mathematics* 50: 1645–1662.

Miyamoto H, Schaal S, Gandolfo F, Gomi H, Koike Y, Osu R, et al. (1996) A Kendama learning robot based on bi-directional theory. *Neural Networks* 9: 1281–1302. http://www.sciencedirect.com/science/article/B6T08-3TDPYNM-22/2/778443608d4a29805a6710a99e175730.

Morimoto J, Endo G, Nakanishi J and Cheng G (2008) A biologically inspired biped locomotion strategy for humanoid robots: Modulation of sinusoidal patterns by a coupled oscillator model. *IEEE Transactions on Robotics* 24: 185–191.

Petric T, Gams A and Zlajpah L (2009) Modeling and control strategy for robotic Powerball. In *18th International Workshop on Robotics*, Alpe-Adria-Danube Region, Brasov, Romania, 25–27 May 2009.

Petrič T, Curk B, Cafuta P and Žlajpah L (2010) Modeling of the robotic powerball: a nonholonomic, underactuated, and variable structure-type system. *Mathematical and Computer Modelling of Dynamical Systems* DOI: 10.1080/13873954.2010.484237.

Pikovsky A, Rosenblum M, Kurths J and Hilborn RC (2002) Synchronization: A universal concept in nonlinear science. *American Journal of Physics* 70: 655–655. http://link.aip.org/link/?AJP/70/655/1.

Righetti L, Buchli J and Ijspeert AJ (2006) Dynamic Hebbian learning in adaptive frequency oscillators. *Physica D* 216: 269–281.

Righetti L and Ijspeert A (2006) Programmable central pattern generators: an application to biped locomotion control. In *Proceedings 2006 IEEE International Conference on Robotics and Automation. ICRA 2006*, pp. 1585–1590.

Ronsse R, Lefevre P and Sepulchre R (2007) Rhythmic feedback control of a blind planar juggler. *IEEE Transactions on Robotics* 23: 790–802.

Ronsse R, Vitiello N, Lenzi T, van den Kieboom J, Carrozza M and Ijspeert A (2010) Human–robot synchrony: flexible assistance using adaptive oscillators. *IEEE Transactions on Biomedical Engineering* 99: 1.

Sato T, Hashimoto M and Tsukahara M (2007) Synchronization based control using online design of dynamics and its application to human–robot interaction. In *IEEE International Conference on Robotics and Biomimetics, 2007. ROBIO 2007*, pp. 652–657.

Schaal S and Atkeson C (1993) Open loop stable control strategies for robot juggling. In *Proceedings 1993 IEEE International Conference on Robotics and Automation*, pp. 913–918.

Schaal S, Mohajerian P and Ijspeert A (2007) Dynamics systems vs. optimal control – a unifying view. *Progress in Brain Research* 165: 425–445. DOI: 10.1016/S0079-6123(06)65027-9.

Sciavicco L, Siciliano B and Sciavicco B (2000) *Modelling and Control of Robot Manipulators*, 2nd edn. New York: Springer-Verlag Inc.

Sentis L, Park J and Khatib O (2010) Compliant control of multicontact and center-of-mass behaviors in humanoid robots. *IEEE Transactions on Robotics* 26: 483–501.

Spong M (1995) The swing up control problem for the acrobot. *IEEE Control Systems Magazine* 15: 49–55.

Spong M and Bullo F (2005) Controlled symmetries and passive walking. *IEEE Transactions on Automatic Control* 50: 1025–1031.

Strogatz SH (1986) *The Mathematical Structure of the Human Sleep–Wake Cycle*. New Yok: Springer-Verlag Inc.

Strogatz SH (1994) *Nonlinear Dynamics and Chaos: With Applications To Physics, Biology, Chemistry, And Engineering* (*Studies in Nonlinearity*). Perseus Books Group.

Thompson SE and Patel RV (1987) Formulation of joint trajectories for industrial robots using b-splines. *IEEE Transactions on Industrial Electronics* 34: 192–199.

Tsuda S, Zauner K-P and Gunji Y-P (2007) Robot control with biological cells. *Biosystems* 87: 215–223.

Ude A, Atkeson CG and Riley M (2000) Planning of joint trajectories for humanoid robots using b-spline wavelets. In *Proceedings of ICRA*, pp. 2223–2228.

van der Pol B (1934) The nonlinear theory of electric oscillations. *Proceedings of the Institute of Radio Engineers* 22: 1051–1086.

Veskos P and Demiris Y (2005) Developmental acquisition of entrainment skills in robot swinging using van der Pol oscillators. *Lund University Cognitive Studies* 123: 87–93. http://cogprints.org/4969/.

Žlajpah L (2006) Robotic yo-yo: modelling and control strategies. *Robotica* 24: 211–220.

Williamson M (1999) Designing rhythmic motions using neural oscillators. In *Proceedings. 1999 IEEE/RSJ International Conference on Intelligent Robots and Systems. IROS '99*, Vol. 1, pp. 494–500.

Williamson MM (1998) Neural control of rhythmic arm movements. *Neural Networks* 11: 1379–1394.

Appendix: Index to Multimedia Extensions

The multimedia extension page is found at http://www.ijrr.org

Table of Multimedia Extensions

Extension	Type	Description
1	Video	Playing yo-yo with either the force feedback or the visual feedback
2	Video	Accelerating gyroscopic device with the robot
3	Video	Synchronizing robot movement to an electromyography (EMG) signal